NACA

RESEARCH MEMORANDUM

ADAPTATION OF A CASCADE IMPACTOR TO FLIGHT MEASUREMENT OF DROPLET SIZE IN CLOUDS

By Joseph Levine and Kenneth S. Kleinknecht

Lewis Flight Propulsion Laboratory
Cleveland, Ohio

NATIONAL ADVISORY COMMITTEE
FOR AERONAUTICS

WASHINGTON
September 18, 1951

NATIONAL ADVISORY COMMITTEE FOR AERONAUTICS

RESEARCH MEMORANDUM

ADAPTATION OF A CASCADE IMPACTOR TO FLIGHT MEASUREMENT OF DROPLET SIZE IN CLOUDS

By Joseph Levine and Kenneth S. Kleinknecht

SUMMARY

A cascade impactor, an instrument for obtaining the size distribution of droplets borne in a low-velocity air stream, was adapted for flight cloud droplet-size studies. The air containing the droplets was slowed down from flight speed by a diffuser to the inlet-air velocity of the impactor.

The droplets that enter the impactor impinge on four slides coated with magnesium oxide. Each slide catches a different size range. The relation between the size of droplet impressions and the droplet size was evaluated so that the droplet-size distributions may be found from these slides. The magnesium oxide coating provides a permanent record of the droplet impression that is not affected by droplet evaporation after the droplets have impinged.

INTRODUCTION

Accurate measurements of droplet-size distribution and liquid-water content are necessary for a more detailed knowledge of heat requirements in de-icing equipment for aircraft operation in icing conditions. In the field of icing research, the rotating multicylinder method (references 1 and 2) has been almost exclusively applied to droplet-size measurement in icing clouds, except for variations based on the same fundamental principle. As a method of evaluating the relative severity of icing, the rotating multicylinder method is quite adequate because a cylinder collects ice in about the same way that an airfoil leading edge collects it. As a means of determining average droplet size and droplet-size distribution in icing clouds, the accuracy of the rotating multicylinder method is questionable because no independent check has been made of the method. Furthermore, the procedure for determining droplet-size distribution is somewhat rough and subjective because it involves fitting the observed data to one of several theoretical curves which lie quite close together.

An instrument that could measure droplet-size distribution and liquid-water content under all conditions and with greater accuracy than the multicylinder method would both improve the data available to designers of de-icing equipment and make basic information available to meteorologists concerning the physics of clouds. A cascade impactor, similar to one described in reference 3, has been successfully adapted at the NACA Lewis laboratory for use in an airplane traveling at a speed in the neighborhood of 100 miles per hour. The adaptation consists in building a diffuser around the cascade impactor to slow down the air from flight speed to that of the air entering the impactor inlet.

The cascade impactor, like the rotating multicylinder, relies on inertia to separate droplets from the air stream according to size, but the method of obtaining droplet-size distributions from the impactor is more direct. The droplets are caught on slides in the impactor and may be observed directly in a microscope. A magnesium oxide coating on the slides is used to obtain permanent impressions of the collected droplets (references 3 and 4). Evaporation of the droplets is therefore permissible. In its adapted form, the cascade impactor is a simple instrument for evaluating cloud droplet-size distribution and liquid-water content.

APPARATUS

Cascade impactor. - A cross section of the cascade impactor is shown in figure 1. It consisted of four stages labeled A, B, C, and D. Air was drawn through the intake by maintaining an exhaust pressure less than one-half the intake pressure. At each magnesium oxide coated slide, a 90° turn in the air flow occurred. The jet air velocities directed at the slides increased as the air traveled from A to D. At stage A, only the largest droplets had sufficient inertia to impinge on the slide. The slides opposite jets B, C, and D in turn caught droplets of smaller and smaller average droplet size because the jet air velocities increased from A to D; that is, the impactor resolved the droplet-size spectrum in the air stream into four narrow droplet-size ranges on the slides. If the droplet-size distribution in the air entering the impactor was narrow, the droplets would be caught principally in one or two stages. If most of the droplets were large, they would be caught principally on the slides of jets A and B. Similarly, if small droplets were prevalent, slides of the C and D jets would catch most of the droplets. The impactor could therefore be used to measure the average droplet size and the breadth of the droplet-size distribution in sprays from nozzles and in clouds.

Flight installation. - The diffuser (fig. 2) is employed to reduce the incoming airspeed from flight speed to that of the air entering the impactor inlet. The streamlines of the air flow entering the impactor

are practically straight so that impingement of droplets on the impactor inlet wall on account of streamline curvature is reduced to a minimum. Attached to the straight section of the diffuser is a hollow strut through which the impactor may be inserted. The diffuser inlet consists of a short straight section 2 inches long and 1 by 1 inch in cross section. The diffuser outlet opening can be varied by two adjustable flaps to control the inlet-air velocity. The outlet opening is adjusted to provide an inlet-air velocity equal to the flight velocity. This adjustment provides straight flow and prevents the inertia separation of droplets that occurs in the presence of curved streamlines. The diffuser was mounted on the bottom of the fuselage of an airplane so that the impactor can be inserted through a hole in the bottom of the fuselage in flight. The arrangement of the impactor mounting in the strut is such as to seal off the diffuser from the interior of the plane. This arrangement was found necessary in order to prevent modification of the flow in the diffuser by leakage of air from the diffuser into the cabin of the plane, because the static pressure in the diffuser is greater than the cabin pressure in flight.

For flight-use of the impactor, a vacuum system of 4-cubic-feet-per-minute capacity was mounted in the airplane (fig. 3). A normally closed solenoid valve was placed in the line between the impactor and the vacuum system; two small surge tanks with a total volume of about 1/2 cubic foot were placed in the line between the valve and the vacuum system. The apparatus was so arranged that the impactor could be loaded with slides from the interior of the airplane and consequently more than one exposure could be made during a flight.

PROCEDURE

Preparation of slides. - Because water and the liquids in sprays are generally volatile, a method for obtaining permanent impressions of the droplets impinging on a slide had to be found. A technique involving the use of slides with a magnesium oxide coating, thin compared with droplet diameter, was found satisfactory. Magnesium oxide coated slides were prepared by burning strips of magnesium approximately 1 inch long under slides that had been cleaned with potassium dichromate - sulfuric acid solution and washed finally with detergent - distilled water solution. The coated slides, when exposed in the impactor and then examined in a microscope with bright-field illumination and a magnification of 100 or 200, show the droplet impressions to be circular with relatively dark central spots and narrow bright rings surrounding each of them (fig. 4).

This magnesium-oxide-coated slide technique differs in detail from the method and the results described in references 3 and 4. In the

technique of references 3 and 4, the magnesium oxide coating of the slide is made approximately as thick as the impinging droplets. The droplet impressions in this case appear as round bright spots or holes in the magnesium oxide coating.

The thinner coating used in the method of this report gives the results described earlier and represents an improvement over the method of references 3 and 4 in that droplets as small as 4 microns leave recognizable impressions as compared with a lower limit of 10 microns in the method of reference 4. In the study of clouds, the detection of droplets less than 10 microns in diameter is important.

Physical nature of droplet impressions. - The difference between the droplet impressions obtained by impingement on relatively thick and on thin magnesium oxide films can be explained qualitatively by examining the collision process in detail (reference 5). A droplet on collision with an uncoated slide surface flattens out into an oblate spheroid with a diameter somewhat greater than the original spherical diameter. In the process, the kinetic energy of the droplet is converted to potential energy of distortion. In other words, work is done against surface tension in increasing the surface area of the droplet. After the droplet has reached its maximum diameter it contracts, perhaps with a few oscillations, to a final equilibrium position. If a thin magnesium oxide coating is on the slide surface, the foregoing description of the impingement process still holds. The outside diameter of the droplet impression corresponds to the greatest diameter of the flattened droplet. The droplet wets the magnesium oxide particles immediately under it and as it contracts pulls the wetted particles with it. After the droplet evaporates, the magnesium oxide contained within the droplet is left behind as a dark spot surrounded by a bright ring relatively free of magnesium oxide. A droplet that hits a relatively thick magnesium oxide coating does not flatten much but leaves a crater, similar to that left by impingement of a rain drop on a snow surface. The holes appear in the microscope as bright spots.

Ratio of droplet diameter to slide impression diameter. - Although the diameters of the droplet impressions are easily measured, the relation between these diameters and the spherical droplet diameters must be determined. A method of evaluating spherical diameter from flattened diameter of droplets caught on a clear slide is given in reference 3. In this case, the equilibrium between gravitational and surface-tension forces results in the flattening. If water droplets did not evaporate so rapidly, the average spherical droplet diameter caught by each stage from a given water spray could be evaluated from water droplets caught on clear slides. Then for the same spray the average impression diameter on magnesium oxide coated slides could be evaluated for each stage.

Unfortunately, the simple and direct method cannot be applied easily because of evaporation of the water. An easier method, not as exact, was devised for handling this problem. Instead of a water spray, a dibutylphthalate spray was used to obtain droplet samples on clear slides because dibutylphthalate has a very low vapor pressure and has the same density as water. The dibutylphthalate spray had a wide droplet-size distribution such that a sample obtained by the impactor was distributed on slides of all four stages. A water spray that was sampled by the impactor loaded with magnesium oxide coated slides likewise had a wide droplet-size distribution such that the sample was distributed among all four stages also. Thus, the droplet-size ranges caught by the B and C stages must have been very nearly the same in the samples from the two sprays on account of the width of the droplet-size distributions and the equal densities of water and dibutylphthalate. The A and D stages cannot be compared in this way because the droplet-size ranges caught on these two stages are not necessarily the same for the two sprays. The only available expedient is therefore to evaluate the ratio of average spherical droplet diameter to average impression diameter for the B and C stages. Then the ratios determined for these two stages may be applied to the A and D stages by virtue of the following qualitative reasoning:

The maximum degree that a droplet is flattened by impact is a function of its size and impact velocity, that is, the ratio of the minor axis to the major axis of a flattened droplet decreases with increasing size and velocity of the droplet. This ratio at least tends to remain constant because of the increase in air jet velocity and decrease in droplet size from stage A to stage D. The magnesium oxide impressions therefore must bear approximately the same proportionality to spherical droplet sizes over all the stages of the impactor.

A simplification of the method of reference 3 can be applied to the determination of spherical diameters from the measured diameters of dibutylphthalate droplets on clear slides. The droplets on the slides have a lens-like vertical cross section (fig. 5); the measured diameters are much greater than the diameters of the corresponding spherical droplets. The focal length of the lens formed by a droplet may be found with the aid of a microscope that has a scale on the fine focal-adjustment knob. The droplet lens forms an image of the illuminated concave mirror situated about 3 centimeters below the microscope slide. After the microscope has been focused on the slide surface, the image of the illuminated mirror formed by the droplet lens may be brought into focus by raising the microscope objective a little with the fine focal adjustment. The difference between the initial fine-focal scale reading and the final one yields the focal length because the object distance is large compared with the image distance. The image of the concave mirror appears as a round bright spot.

From the focal length f of the droplet lens and the index of refraction n of dibutylphthalate, the radius of curvature r of the lens may be determined from the thin lens equation

$$r = (n - 1)f$$

From the geometry of the lens, the radius of the spherical droplet having the same volume as the lens may be computed. The computation of spherical droplet size from focal length is described in appendix A.

With the aid of the foregoing method and some measurements of focal lengths, the relation between measured diameter and droplet diameter before impingement was established. The focal lengths of 37 dibutylphthalate droplet lenses, which ranged in diameter from 151.3 to 8.7 microns, were measured. The values of focal length are plotted against the diameter in figure 6 and a smooth curve is drawn through the scattered points. With the aid of equations (A1) to (A4) in appendix A, several points on the curve of figure 6 were converted to actual droplet diameter from which a curve of actual diameter against measured diameter was constructed (fig. 7). Then the average true droplet diameters corresponding to stages B and C, respectively, were obtained from the dibutylphthalate droplets. The average magnesium oxide impression diameters of the B and C stages were obtained from the water-droplet impressions from which the ratio of average actual diameter to impression diameter was calculated. The ratios obtained for the B and C stages differ slightly so that an average value of 0.713 was adopted. Thus, the relation of impression diameter to droplet diameter is determined approximately.

Method of obtaining frequency distributions. - Droplet-size frequency distributions were obtained of the droplets caught on each slide and then combined to yield the total distribution. This procedure was the most accurate way of obtaining the frequency distribution from a droplet sample made by the impactor, but this procedure is so laborious that it has only been applied to a sample with a low droplet density per unit area of slide. A filar-eyepiece micrometer was used to measure impression diameters and a vernier on the stage for moving the slide was used to traverse strips, having a width the same as the field of view, so that the entire area of the slide was traversed. The frequency distributions of each stage were subsequently obtained and added to yield the complete frequency distribution.

If the droplet sample is dense enough, a less laborious but less exact procedure may be used. If the less exact procedure is followed, photomicrographs of several typical areas on a slide may be made, but care must be taken that fair sample areas are chosen. When the examination of the impingement areas on many slides was made, apparently most

of the droplets were concentrated in an area that was roughly the projection of the cross-sectional area of the jet. The droplets were concentrated more along the edges of the impingement area with the downstream edge favored more than any of the other edges. The concentration towards the edges of the impingement area increased from stage A to stage D. The ratio of the relatively low-density central area to the more highly concentrated area near the edges of a given impingement area was estimated to be 3:2 for all stages. Therefore, five areas were chosen as indicated in figure 8. The cross-sectional areas of the jets decreased from stage A to stage D causing the principal area of droplet impingement to decrease in size from stage A to stage D. The droplets caught by each successive stage were therefore concentrated in a smaller area from stage A to stage D. Consequently, the droplet counts of each stage must be multiplied by a factor proportional to the area of impingement, which is roughly equal to the jet area. After multiplication by the appropriate factor, the corrected droplet counts of each stage may be added, as in the more exact procedure, to yield the complete frequency distribution.

RESULTS AND DISCUSSION

The impactor-diffuser combination was used successfully on three flights. The cloud droplet-size distributions measured during the three flights are summarized in figures 9 and 10 in the form of normalized histograms. The width of a step on the histogram represents a definite droplet-diameter range, and the height of a step is proportional to the number of droplets within that particular size range. These histograms were normalized with the formula

$$H = \frac{n}{WN}$$

where H is the normalized step height, W the step width in microns, n the number of droplets in the size range W, and N the total number of droplets constituting the droplet-diameter frequency distribution. Normalization makes possible the direct graphical comparison of frequency distributions with different values of N.

Results from two flights with the impactor-diffuser alone are shown in figure 9. The first flight was made at a temperature above freezing in thick stratiform clouds. Occasional light rain was observed during the flight. The second flight was made in a relatively thin layer of strato-cumulus cloud at a temperature below freezing. Light icing of the airplane and diffuser inlet occurred during this flight, but the icing evidently was not severe enough to interfere with the operation of the instrument. The lower sampling time for the first flight indicated in figure 9 was a consequence of the higher droplet density. Apparently, from inspection of figure 9, the higher droplet density was also associated with a slightly greater average droplet size.

Gravitational settling of droplets within the diffuser may be the cause of appreciable errors in the sampling of large droplets. The effect of gravity on droplet trajectories within the diffuser has been evaluated, and the results are presented in figure 11. The method of computation for droplet trajectories is presented in appendix B. Droplets larger than 30 microns in diameter apparently settle out quite markedly in the diffuser before the impactor is reached (fig. 11). Therefore, the impactor-diffuser combination in its present form cannot evaluate accurately droplet size distributions extending above 30 microns; however, a comparison with a droplet camera that supports the validity of samples obtained by the impactor-diffuser combination in the range below 30 microns has been made.

A third flight was made with the impactor diffuser and with a cloud droplet camera (reference 6) operating simultaneously. Because the droplets are photographed as they occur in the atmosphere, the camera is not subject to any wall losses, but the camera is so limited in field of view that adequate cloud samples are not easily obtained. Nevertheless, a successful comparison in flight of the impactor diffuser with the cloud droplet camera was made on a day when fair-weather cumulus clouds were plentiful. The histograms of the droplet-size distributions obtained by the two instruments apparently agree quite well as shown in figure 10. In the photographs no droplets larger than 30 microns in diameter appeared. Thus, the camera and impactor diffuser apparently agree in the droplet-size range which the impactor diffuser can handle.

CONCLUDING REMARKS

From the experience gained with the present impactor-diffuser combination, the diffuser as used in its present form apparently is the factor that determines the upper limit of proper droplet-size distribution measurement. Droplet trajectory computations showed that the present diffuser causes an appreciable loss of droplets greater than 30 microns because the cloud droplets in the diffuser suffer gravitational settling. The length of the diffuser section could be shortened by about 30 percent so that droplets as large as 100 microns would not have settled out appreciably by the time the end of the diffuser section has been reached. Furthermore, the length of the straight section should be decreased so that the mouth of the impactor is as close to the end of the tapered diffuser section as possible. The impactor in turn must be modified to adapt it to the higher diffuser velocity.

In order to adapt the impactor diffuser for use in severe icing conditions provisions may be made for de-icing the inlet.

Lewis Flight Propulsion Laboratory
National Advisory Committee for Aeronautics
Cleveland, Ohio

APPENDIX A

EVALUATION OF TRUE DIAMETER FROM DROPLET-LENS DIAMETER

The spherical radius of an impacted droplet having a lens-like shape may be determined by the following method: From the lens equation

$$r = (n-1)f \tag{A1}$$

and the measured focal length of a droplet lens, it is possible to compute the radius of curvature r of the lens. The height of the lens h is related to r and the lens diameter $2a$ by

$$h = r\left(1 - \sqrt{1 - \frac{a^2}{r^2}}\right) \tag{A2}$$

and the volume v of the lens is

$$v = \frac{1}{6}\pi h\,(h^2 + 3a^2) \tag{A3}$$

The radius R of the spherical droplet before impaction can be obtained from

$$R = \sqrt[3]{\frac{3v}{4\pi}} \tag{A4}$$

APPENDIX B

COMPUTATION OF DROPLET TRAJECTORIES

The trajectories of droplets within the diffuser are the result of the combined action of aerodynamic drag and gravitation. When a droplet enters the diffuser it encounters an environment of decreasing air velocity. The inertia of the droplet tends to maintain the original velocity. Aerodynamic drag which tends to decrease the difference between droplet and air velocity then arises. Meanwhile, the force of gravity acts to maintain the falling velocity of the droplet.

In order to determine the trajectories of droplets in the interior of the diffuser, the air velocity as a function of position in the tapered portion of the diffuser must be evaluated. For simplicity, the velocity component V_x in the direction of the x-axis is to be considered a function of x, the distance along the diffuser axis of symmetry, alone. With the foregoing simplification, V_x merely depends on the cross-sectional area A of the diffuser at x as expressed by the simple relation

$$V_x = \frac{A_o}{A} V_{o,x} \tag{B1}$$

where A_o is the entrance cross-sectional area and $V_{o,x}$ is the x-component of entrance velocity. The diffuser is so constructed that any cross section perpendicular to the x-axis is a square. If the length of the side of the entrance cross section is s_o and the slope of the diffuser walls is λ, the areas A_o and A can be evaluated in terms of λ, s_o, and x with the following results:

$$V_x = \frac{dx}{dt} = \frac{V_{o,x}}{\left(1 + \frac{2\lambda x}{s_o}\right)^2} \tag{B2}$$

The exact differential equation of motion of a droplet in the foregoing velocity field can be integrated exactly by a differential analyzer or numerical integration. A less exact and less laborious method was devised for handling this problem. The equation of motion of a droplet was solved for the case where a droplet carried by an air stream of velocity V_1 is suddenly projected into an air stream of velocity V_2. The problem of the trajectory of the droplet in the diffuser was solved then by arbitrarily slicing the length

of the diffuser into sections of equal length L (fig. 12). In order to reduce the droplet trajectory problem to the foregoing simple case, a mean value was assigned to the velocity of the air in each section.

The equation of motion of a droplet actually has two components: one in the horizontal or x-direction and the other, which contains the effect of gravity, in the vertical or z-direction. The motion of the droplet in the x-direction is considered first. The velocity of a droplet projected from an air stream of velocity V_1 into a stream of velocity V_2, both moving in the x-direction, is initially $\Delta V_{o,x} = V_{2,x} - V_{1,x}$ with respect to the air of velocity $V_{2,x}$. The equation of motion of the droplet is written as

$$m \frac{d\Delta V_x}{dt} = - 6\pi\mu a \frac{C_D R}{24} \Delta V_x$$

where m is mass, ΔV_x velocity of the droplet relative to the air in the x-direction, μ coefficient of viscosity of air, a radius, C_D drag coefficient, and R Reynolds number. Because the density of water is practically 1, the mass is

$$m = \frac{4}{3} \pi a^3$$

and the equation of motion becomes

$$\frac{d\Delta V_x}{dt} = - \frac{9}{2} \frac{\mu}{a^2} \left(\frac{C_D R}{24} \right) \Delta V_x \tag{B3}$$

By integration the following equations are obtained

$$\begin{aligned} \Delta V_x &= \Delta V_{o,x} \, e^{- \frac{9}{2} \frac{\mu}{a^2} \left(\frac{C_D R}{24} \right) t} \\ &= \Delta V_{o,x} \, e^{- Kt} \end{aligned} \tag{B4}$$

and

$$\Delta x = \frac{\Delta V_{o,x}}{K}\left(1 - e^{-Kt}\right) \tag{B5}$$

where

$$K = \frac{9}{2}\frac{\mu}{a^2}\left(\frac{C_D R}{24}\right)$$

and Δx is the distance the droplet moves relative to the air in time t. The time taken by the droplet to travel the distance L is the quantity desired; but, first, the time taken by an air particle to travel a given distance must be obtained. Integration of equation (B2), yields

$$t = \frac{s_o}{6\lambda V_{o,x}}\left[\left(1 + \frac{2\lambda x}{s_o}\right)^3 - 1\right] \tag{B6}$$

where t is the time taken for an air particle to travel the distance x from the entrance (figs. 11 and 12) along the axis of the diffuser. From equation (B6) the time for an air particle to travel from the entrance to any slice boundary in the diffuser may be computed. If time differences are taken, the time intervals Δt_1, Δt_2, . . . can be computed for an air particle to travel through the first slice, second slice, etc., respectively. The respective average air velocities in each slice are therefore $L/\Delta t_1$, $L/\Delta t_2$, . . . and are the average air velocities used in computing the droplet trajectories.

The trajectory of the droplet in the x-direction must be found by solution of the two simultaneous equations (B5) and (B6); because these equations cannot be solved explicitly, numerical methods must be applied. For example, a droplet entering the first slice has the velocity of the air entering the diffuser, that is, $V_{o,x}$. The average velocity of the air in the first slice is $\bar{V}_{1,x} = L/\Delta t_1$. The average initial velocity difference is $\Delta V_{1,o,x} = V_{o,x} - \bar{V}_{1,x}$ (fig. 12). The Reynolds number is computed from

$$R = \frac{a\rho_a \Delta V_x}{\mu}$$

where ρ_a is the air density and ΔV_x is the velocity of the droplet with respect to the air. The function $C_D R/24$ of R is tabulated in reference 1 so that the value of R can be obtained for substitution in equations (B4) and (B5). The problem is solved by finding values Δx_1 and t_1 satisfying equations (B5) and (B6). During the time t_1, when the droplet travels the distance L in the first slice, an air particle starting out with the droplet travels a distance $L-\Delta x_1$ (fig. 12). By successive approximations, a value of t_1, which is equal to the time taken by an air particle to cover the distance $L-\Delta x_1$ as computed from equation (B6), is obtained. Once t_1 is found, the value of $\Delta V_{1,x} = V_{1,x} - \bar{V}_{1,x}$, which is the average velocity difference at the end of the first slice, is computed from equation (B4). The procedure is continued into the second slice with $\Delta V_{2,o,x} = V_{1,x} - \bar{V}_{2,x}$ and similarly into the remainder of the slices until the untapered portion of the diffuser is reached.

There is some question as to how small the slices should be made. In the computations for this paper, L was chosen to be 10 centimeters. In order to ascertain the reasonableness of the chosen value of L, the first slice was subdivided into smaller slices of 2 centimeters length, and a droplet trajectory was computed. Within the accuracy of the computations, no appreciable difference could be found between the values of $V_{1,x}$ and t, computed in one step as compared with those computed in five steps with $L = 2$ centimeters.

The foregoing method yields the x-coordinate of a droplet as a function of time, but the vertical or z-coordinate of the droplet is yet to be found. The equation of vertical motion of a droplet is

$$m \frac{d\Delta V_z}{dt} = - 6\pi a\mu \left(\frac{C_D R}{24} \right) \Delta V_z + mg$$

where ΔV_z is the velocity of the droplet with respect to the air and g is the acceleration due to gravity. Substitution of $m = \frac{4}{3} \pi a^3$ transforms the equation of vertical motion to

$$\frac{d\Delta V_z}{dt} = - K\Delta V_z + g \tag{B7}$$

Integration of equation (B7) yields

$$\Delta V_z = \frac{d\Delta_z}{dt} = \frac{g}{K} + \left(\Delta V_{o,z} - \frac{g}{K}\right)e^{-Kt} \tag{B8}$$

and

$$\Delta z = \frac{g}{K}t + \frac{1}{K}\left(\Delta V_{o,z} - \frac{g}{K}\right)\left(1 - e^{-Kt}\right) \tag{B9}$$

where Δz is the distance the droplet falls during time t. Equations (B7) and (B8) are applied to the same slices as in the evaluation of droplet trajectories in the x-direction. Velocity components in the z-direction are so small compared to those in the x-direction that R and $C_D R/24$ are evaluated in terms of the x-component of velocity, which is very little different from the absolute magnitude of the actual velocity vector. Therefore K is computed using the values of $C_D R/24$ obtained from the x-components of relative velocity.

With equation (B8) the final relative velocity in the vertical direction was computed from the initial relative velocity of a droplet passing through a slice. Likewise equation (B9) was used to compute the distance through which a droplet would fall in passing through a slice, and the final relative vertical velocity at the end of one slice became the initial relative velocity of the next slice. Only the trajectories of droplets entering the diffuser along its axis of symmetry were computed, and the vertical components of air velocity within the diffuser have been neglected. Allowance for the vertical air-velocity components in the diffuser would have caused the computed droplet trajectories to intersect the diffuser wall a little sooner. For evaluation of the performance of the diffuser, the trajectories as calculated are sufficiently accurate.

REFERENCES

1. Langmuir, Irving, and Blodgett, Katherine B: A Mathematical Investigation of Water Droplet Trajectories. Tech. Rep. No. 5418, Air Materiel Command, AAF, Feb. 19, 1946. (Contract No. W-33-038-ac-9151 with Gen. Elec. Co.)

2. Anon.: The Multicylinder Method. The Mount Washington Monthly Res. Bull., vol. II, no. 6, June 1946.

3. May, K. R.: The Cascade Impactor: An Instrument for Sampling Coarse Aerosols. Jour. Sci. Instruments, vol. XXII, no. 10, Oct. 1945, pp. 187-195.

4. May, K. R.: The Measurement of Airborne Droplets by the Magnesium Oxide Method. Jour. Sci. Instruments, vol. XXVII, no. 5, May 1950, pp. 128-130.

5. Vonnegut, B., Cunningham, R. M., and Katz, R. E.: Report on Instruments for Measuring Atmospheric Factors Related to Ice Formation on Airplanes. Tech. Rep. 5519, Air Materiel Command, AAF, Aug. 13, 1946. (Contract No. W-33-038-ac-5443.)

6. McCullough, Stuart, and Perkins, Porter J.: Flight Camera for Photographing Cloud Droplets in Natural Suspension in the Atmosphere. NACA RM E50K01a.

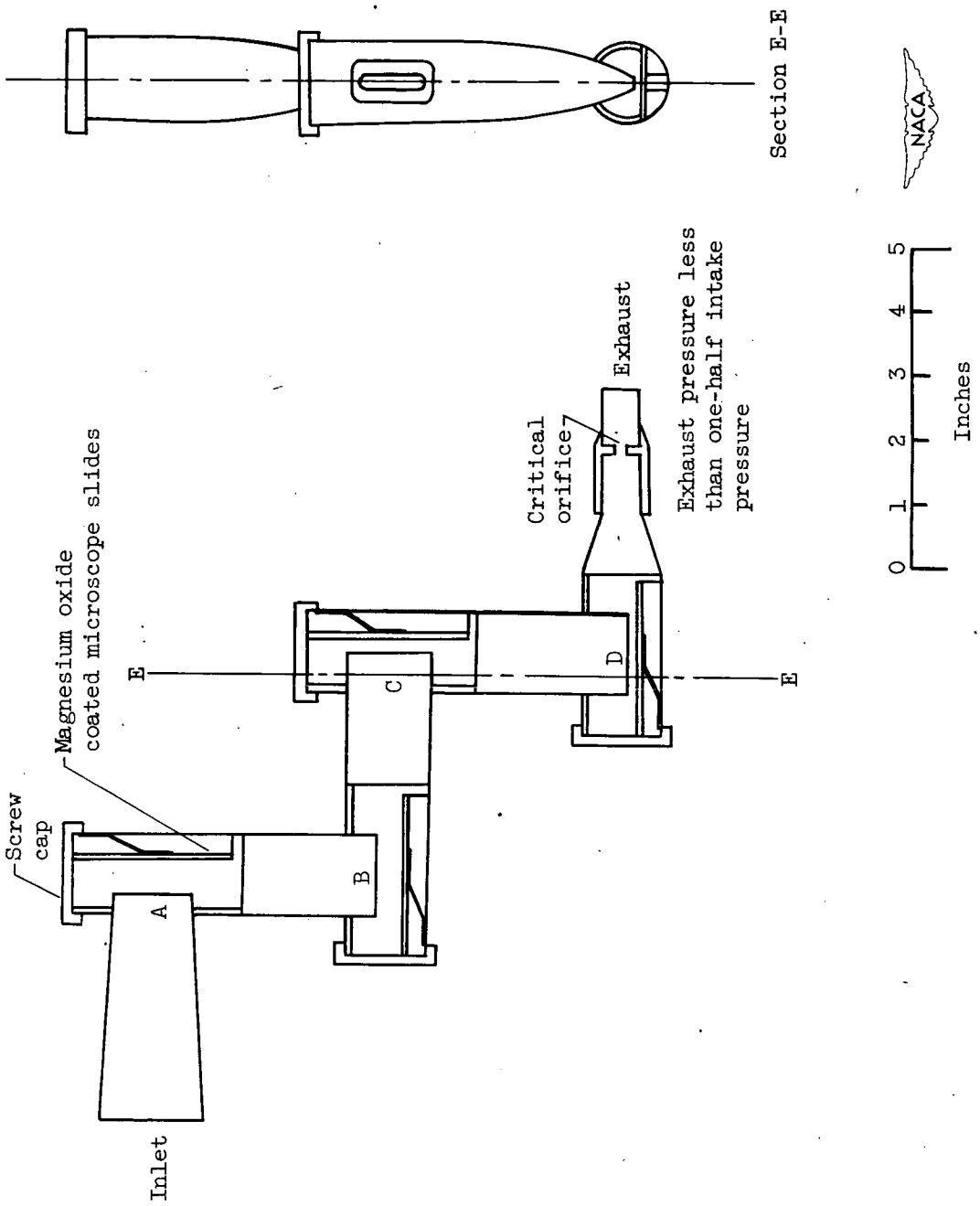

Figure 1. - Cascade impactor.

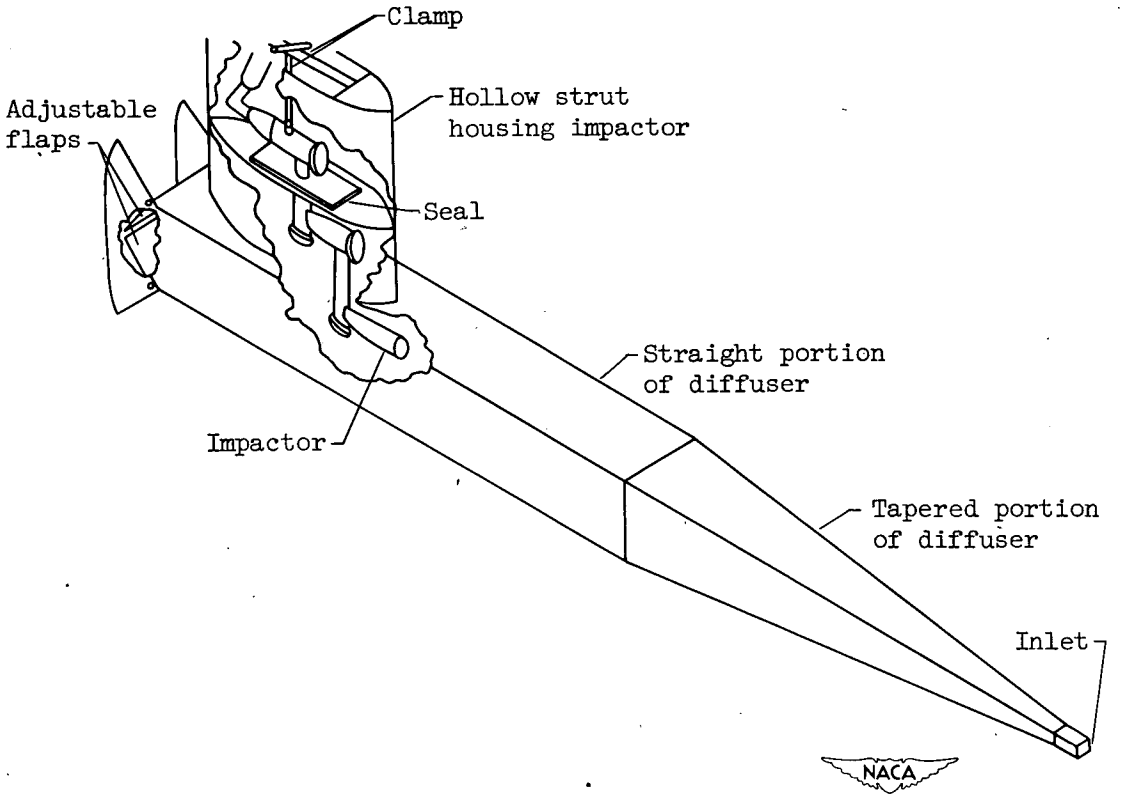

(a) With impactor in operating position.

Figure 2. - Diffuser used to reduce incoming airspeed.

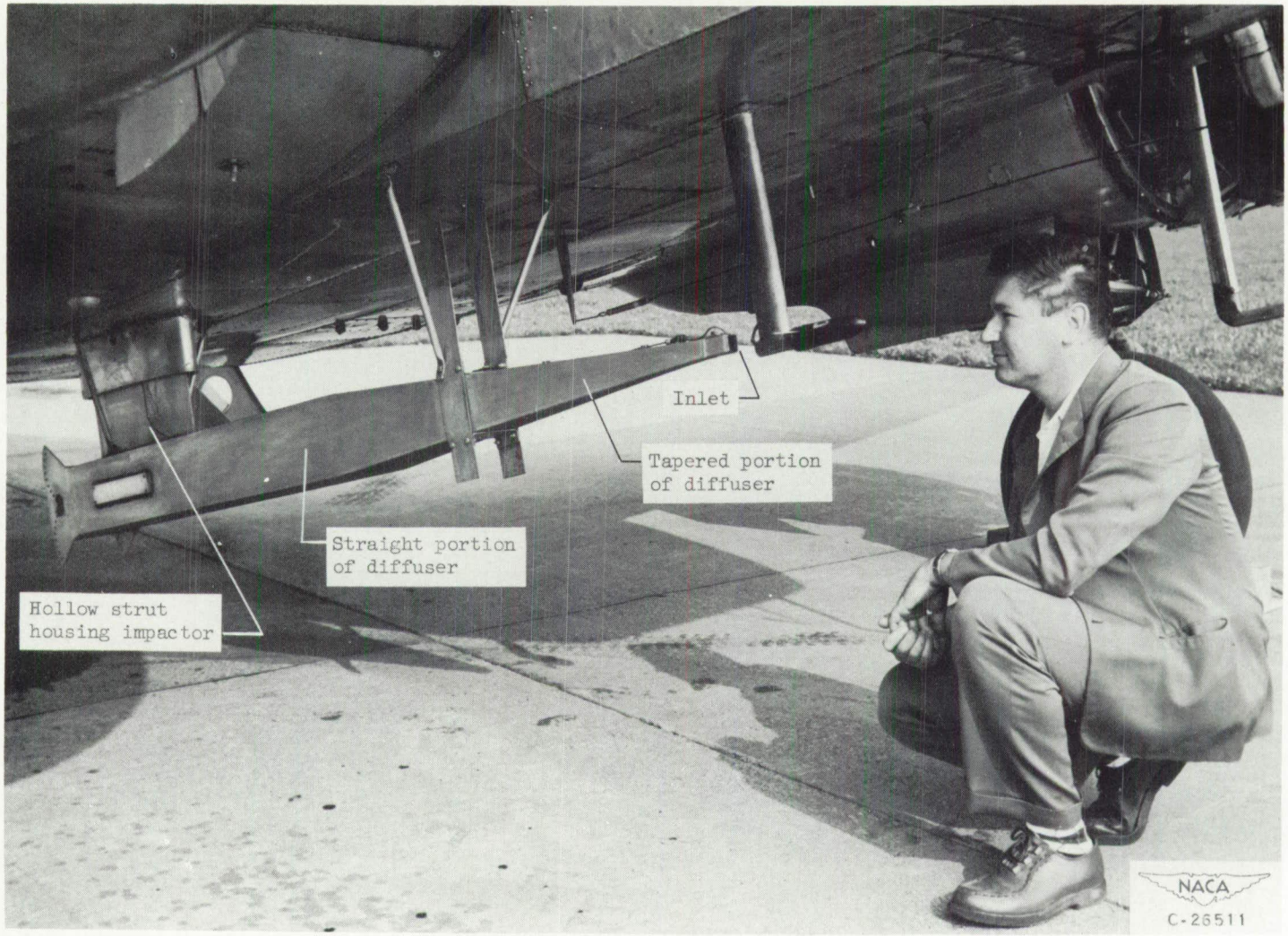

(b) Mounted on airplane; inlet view.

Figure 2. - Continued. Diffuser used to reduce incoming airspeed.

(c) Mounted on airplane; outlet view.

Figure 2. - Concluded. Diffuser used to reduce incoming airspeed.

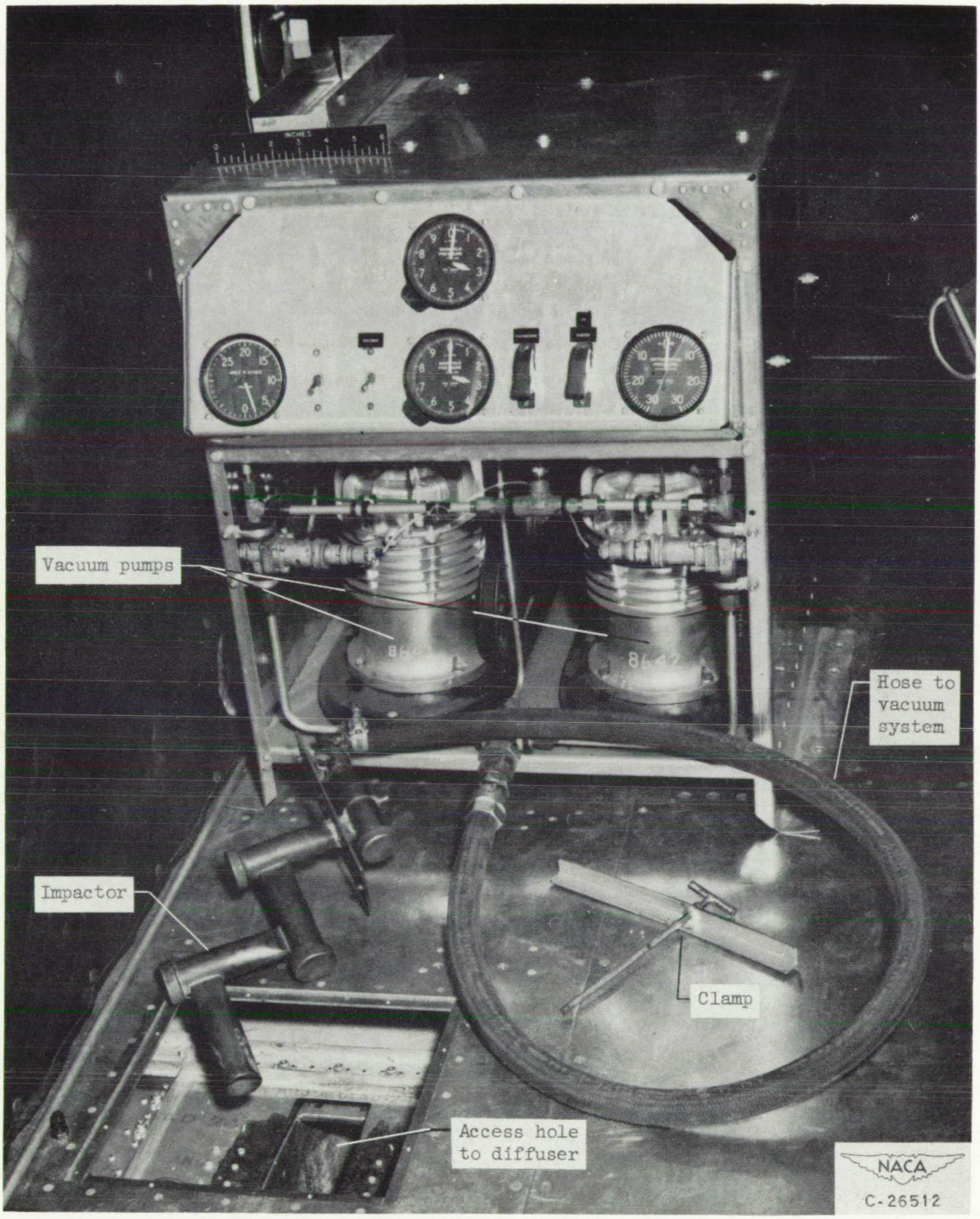

Figure 3. - Installation inside airplane.

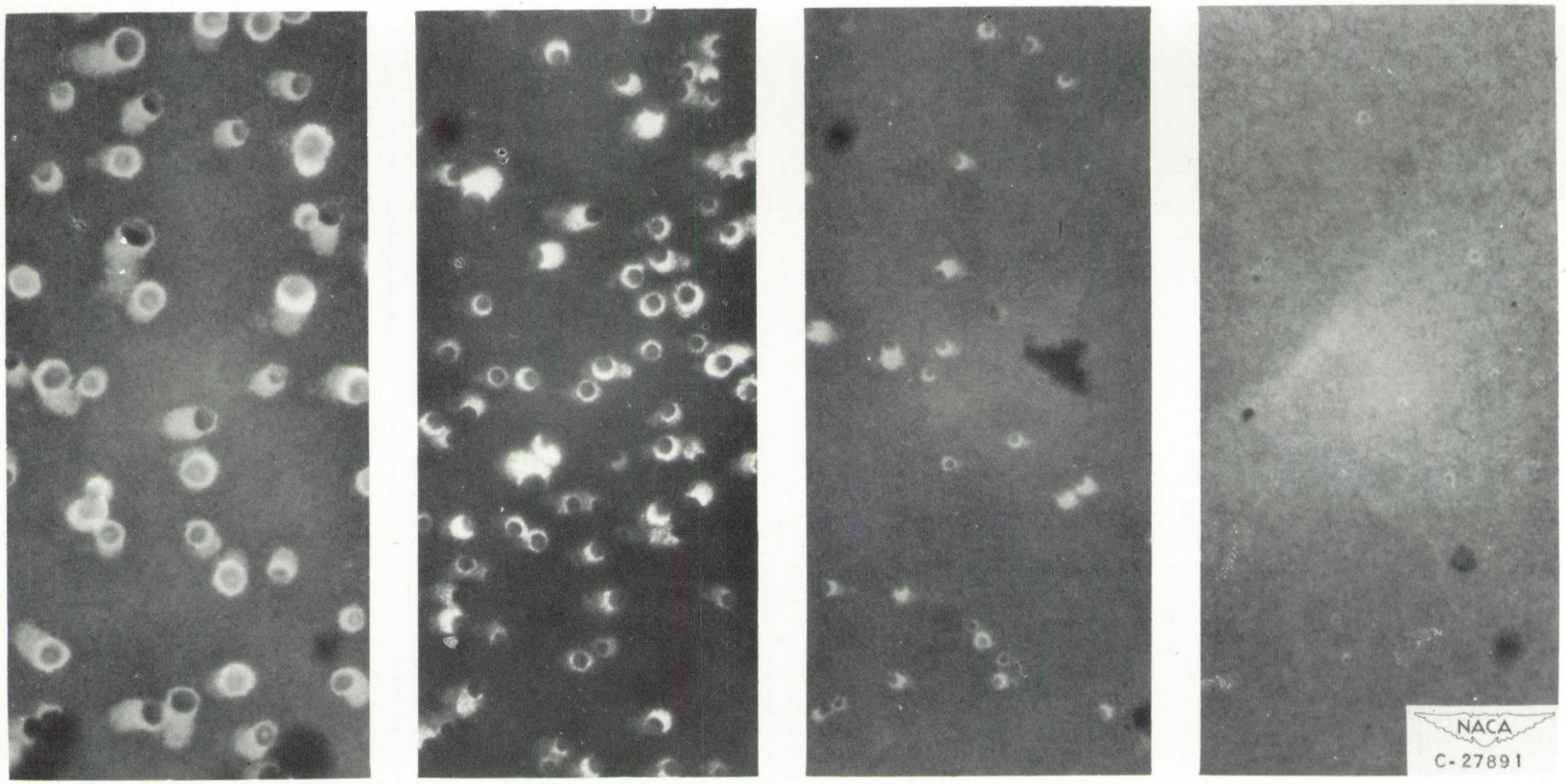

(a) Stage A. (b) Stage B. (c) Stage C. (d) Stage D.

Figure 4. - Photomicrographs of slides exposed in impactor during flight made on January 5, 1950; X164.

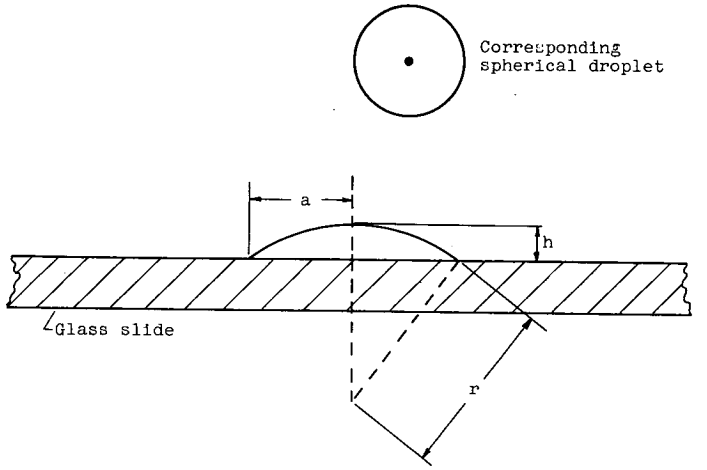

Figure 5. - Cross section of dibutylphthalate droplet lens.

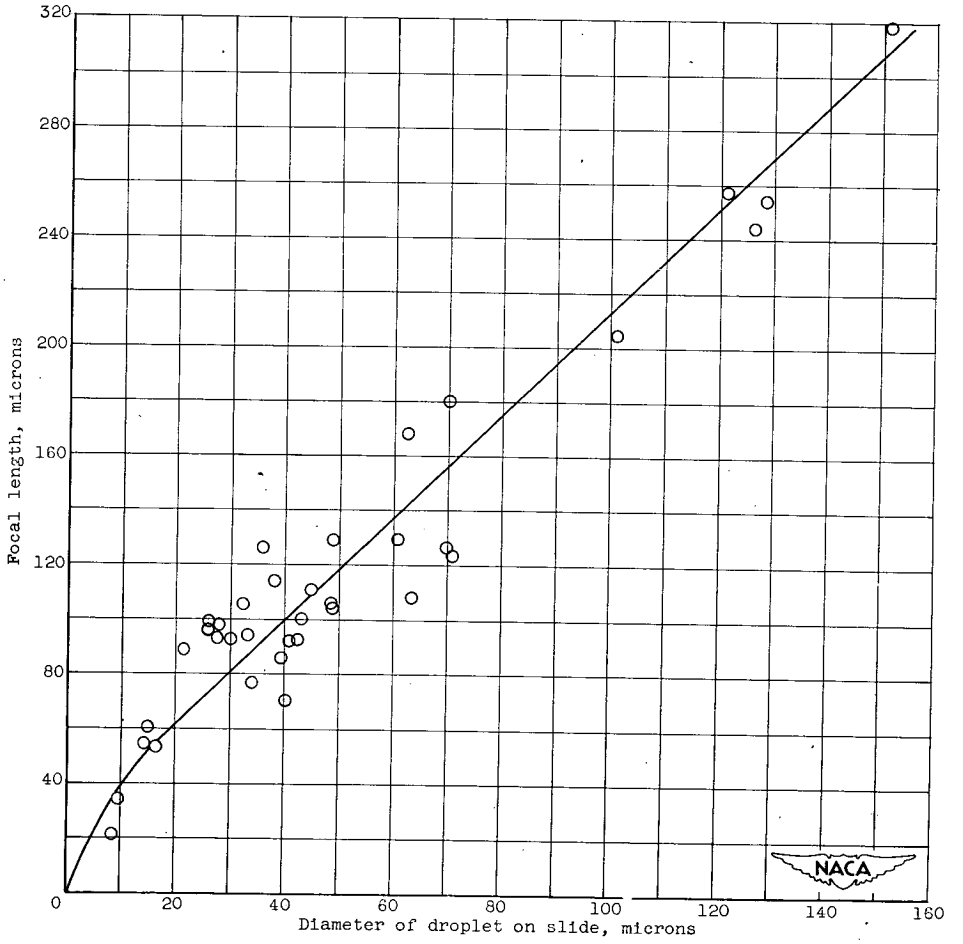

Figure 6. - Focal lengths of dibutylphthalate droplets of various measured diameters.

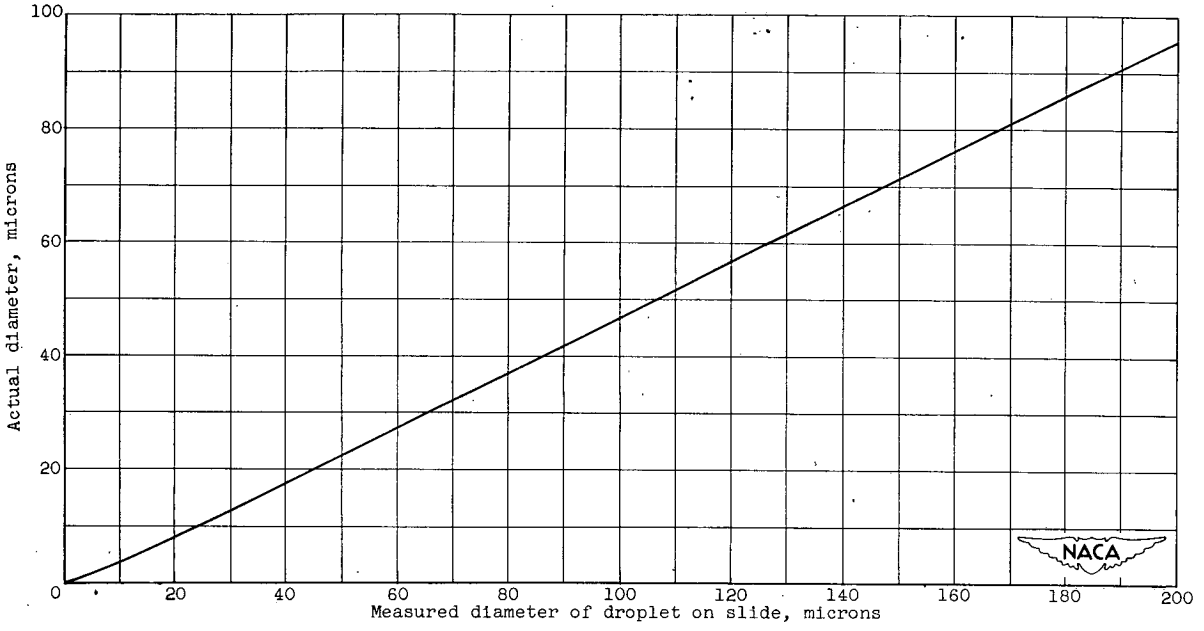

Figure 7. - Actual diameter against measured diameter for dibutylphthalate droplets.

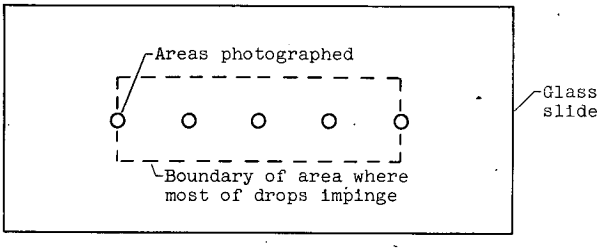

Figure 8. - Diagram of impactor slide showing location of areas at which photomicrographs were taken.

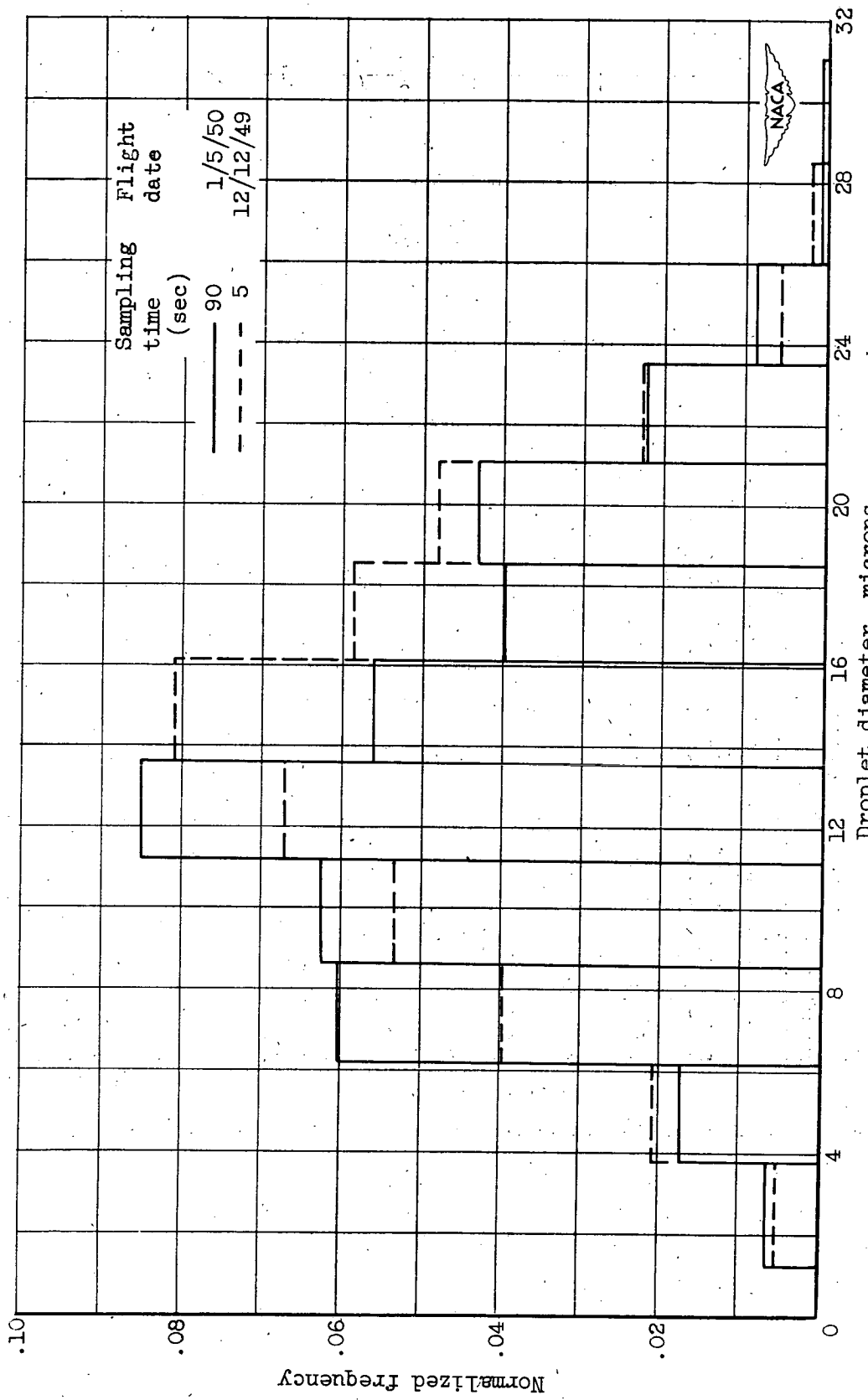

Figure 9. - Normalized droplet-size distribution curves obtained from two flights with impactor.

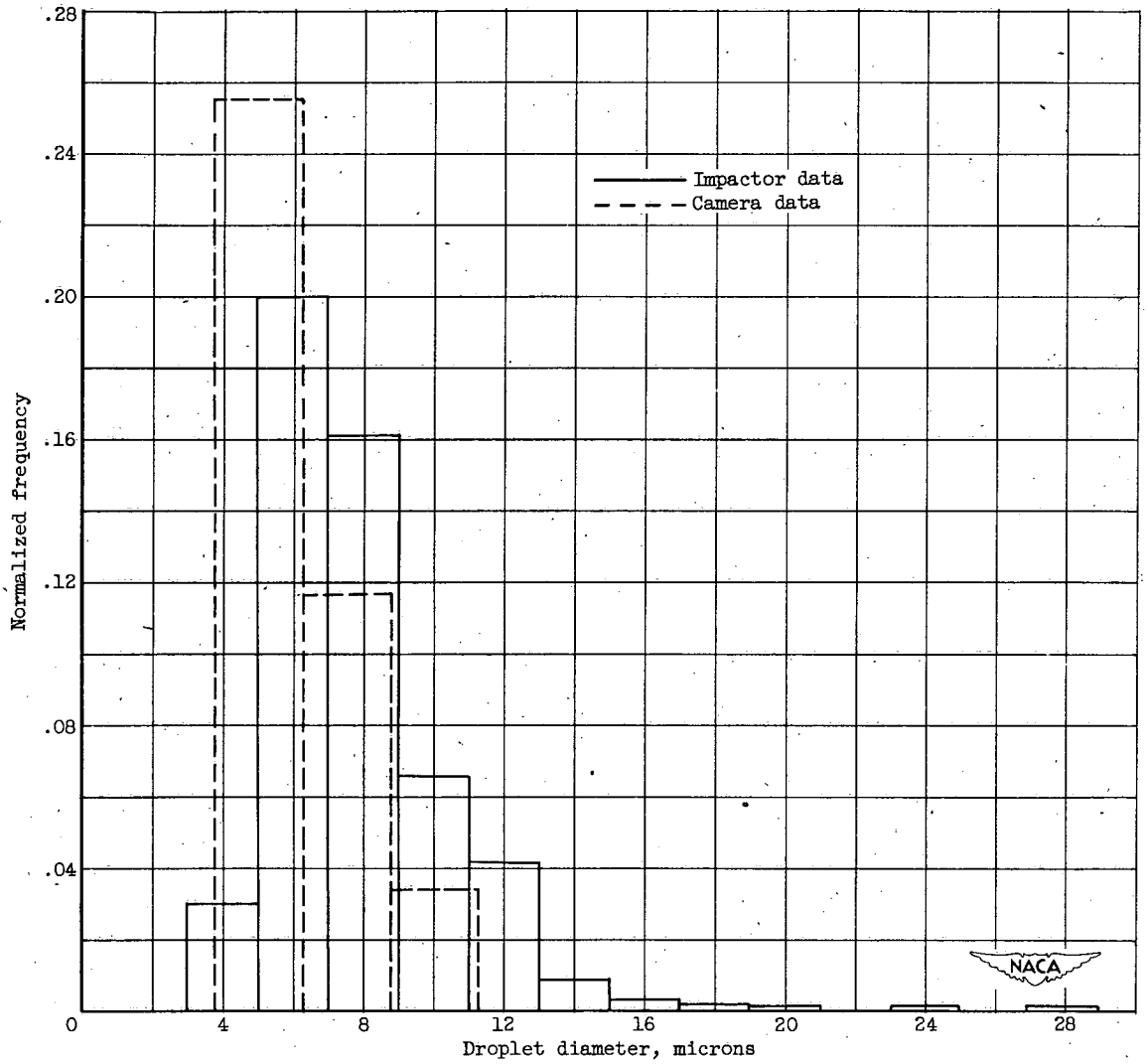

Figure 10. - Comparison of data obtained simultaneously by camera and impactor in flight.

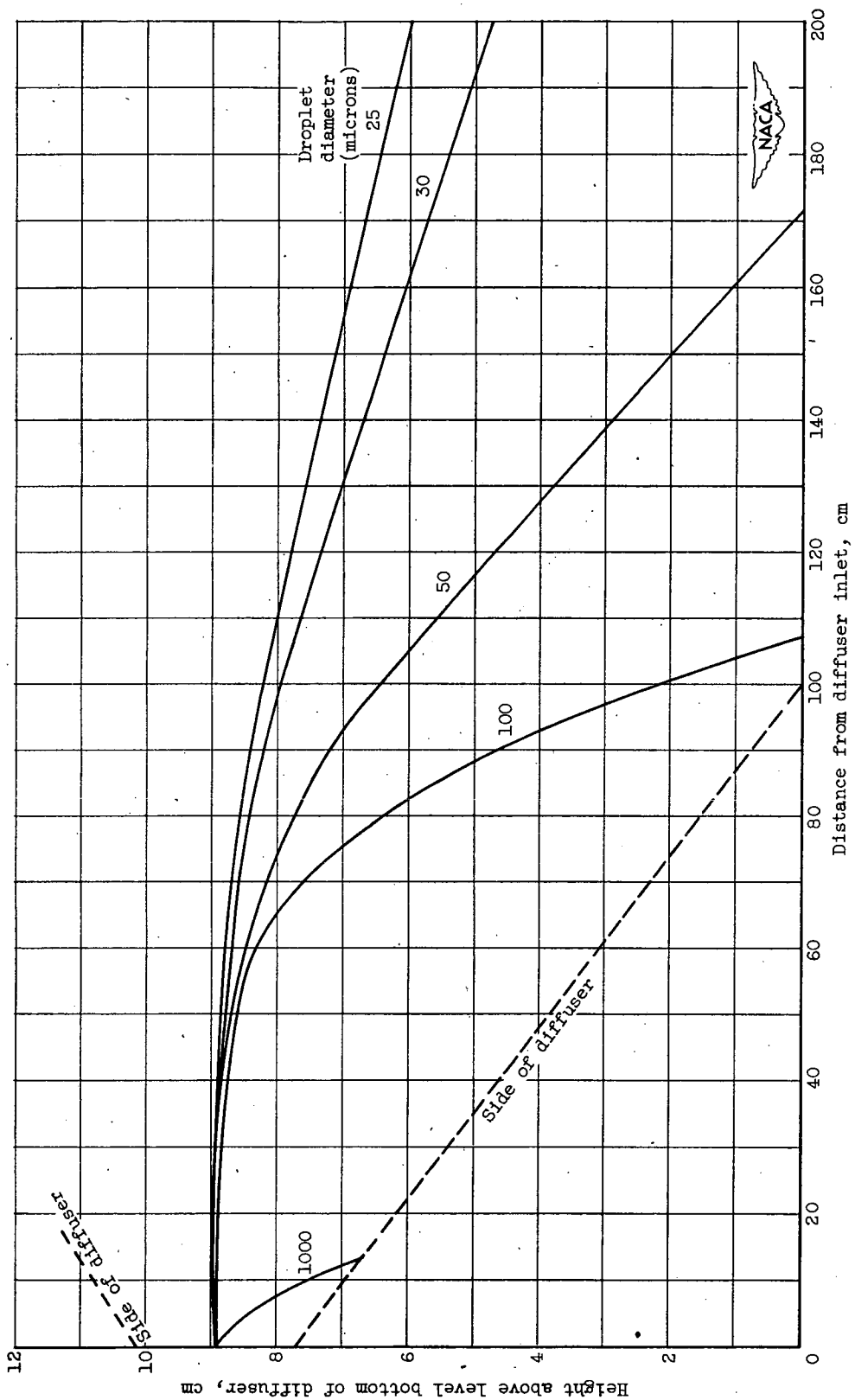

Figure 11. - Droplet trajectories in diffuser; inlet velocity, 100 miles per hour.

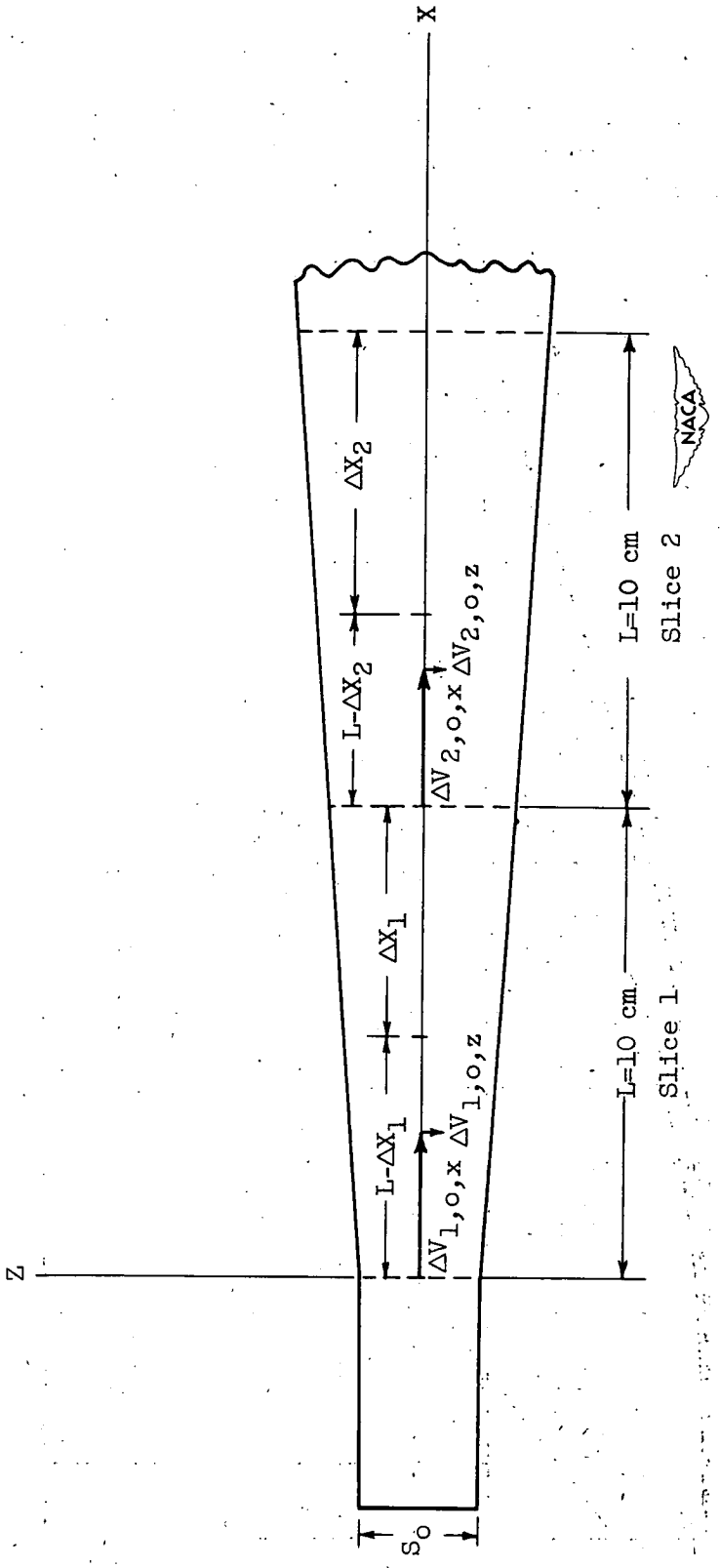

Figure 12.- Diagram of first two slices of diffuser.